Available online at www.sciencedirect.com
SCIENCE DIRECT®

Journal of the European Ceramic Society 24 (2004) 725–732

www.elsevier.com/locate/jeurceramsoc

Reversible and irreversible piezoelectric and ferroelectric response in ferroelectric ceramics and thin films

D. Bolten*, U. Böttger, R. Waser

Institut für Werkstoffe der Elektrotechnik, University of Technology RWTH Aachen, D-52056 Aachen, Germany

Received 5 February 2003; received in revised form 14 April 2003; accepted 27 April 2003

Abstract

In this article, a novel characterization method, the separation between reversible and irreversible contributions, is applied to the piezoelectric and ferroelectric response of ferroelectric ceramics and thin films. The reversible contributions are determined by the measurement of appropriate small-signal properties, e.g. the piezoelectric coefficient for the piezoelectric response and the small-signal capacitance for the polarization response of the material, and compared to the corresponding large signal properties (i.e. the strain–field dependence and polarization–field dependence, respectively). The comparison between thin films and bulk ceramics indicates that the non-180° domain wall motion in ferroelectric thin films is reduced compared to bulk ceramics.
© 2003 Elsevier Ltd. All rights reserved.

Keywords: Dielectric properties; Ferroelectric properties; Piezoelectric properties; PZT

1. Introduction

The origin of the ferroelectric hysteresis is the existence of irreversible processes for higher changes of the driving electric field. For small changes in the driving field, the corresponding changes in the polarization are reversible. The reversible contributions originate from the (dielectric) response of the lattice and from reversible domain wall motions with a small amplitude. An early investigation of reversible domain wall motion in ferroelectrics can be found in Ref. 1.

To the present understanding, there are basically two mechanisms that lead to irreversible changes in the ferroelectric polarization. First, a lattice cell can switch from one thermodynamically stable configuration (say $+P_{sat}$) to another ($-P_{sat}$). The second mechanism is irreversible domain wall motion, elucidated by a simple model based on the assumption that the domain wall is moving through some kind of potential generated by the interaction of the domain wall with randomly distributed defects of the lattice, e.g. dislocations, dopant ions, vacancies, etc.[2–4]

Reversible domain wall motions result when the domain wall is moving inside a local minimum of the random potential. The domain wall contributes irreversibly when the force exerted on the wall by the external field is big enough to drive the domain wall over a local maximum of the potential, thus preventing the wall from returning into its initial position when the external force is removed.

There are three approaches to experimentally obtain information about reversible and irreversible processes: the measurements of Rayleigh-loops, the measurement of recoil curves and the measurement of small-signal properties. For an introduction into this approach, a comparison between those methods and their application to ferroelectrics, the reader is referred to Ref. 5. In this study, the last method has been applied to the piezoelectric and polarization response of ferroelectric thin films and bulk ceramics.

The small signal capacitance (permittivity) is measured by superimposing an AC electric field with a small amplitude (=1 kHz, 50–100 mV) over a (slowly varying) DC field that traces the hysteresis loop. The capacitance is then determined by the measurement of the component of the current that is phase-shifted by 90° with respect to the driving AC voltage. Indeed, the effective slope of a local subcycle is determined in this way. As a

* Corresponding author.
E-mail address: Dierk.Bolton@amtc-dresden.com (D. Bolten).

0955-2219/03/$ - see front matter © 2003 Elsevier Ltd. All rights reserved.
doi:10.1016/S0955-2219(03)00317-0

result one obtains a so-called capacitance–voltage dependence (C–V). In the limit of vanishing amplitude of the applied AC signal, one can expect that the domain walls move only reversibly inside a local minimum of the interaction potential, so that the measured response is a measure for the reversible contribution of the domain walls at a given DC bias (and of the domain configuration at that given DC bias). Since ideally no irreversible processes occur during the measurement of a minor loop (in the limit $E_{ac}\rightarrow 0$), the measurements are made under the condition of constant irreversible polarization P_{irrev}. This approach is very similar to the measurement of the reversible susceptibility used in the study of ferromagnetic materials where the incremental susceptibility $\Delta M/\Delta H$ (i.e. the slope of a minor loop) defines, in the limit of $\Delta H\rightarrow 0$, the reversible susceptibility χ_{rev}.[6]

Since by definition $C=\mathrm{d}Q/\mathrm{d}U$, a polarization can formally extracted from a C–V curve by:

$$P_{rev}=\frac{1}{A}\int C(V)\mathrm{d}V \quad (1)$$

where A denotes the area of the sample. P_{rev} can be interpreted as the reversible polarization contributions along the hysteresis curve, again in complete analogy to the magnetic case.[7] For a more thorough justification of this method, the reader is referred to Ref. 5.

The measurement of the piezoelectric coefficient is the piezoelectric analogue to the measurement of the permittivity. In both cases, a small AC signal is superimposed with a slowly varying DC bias which is used to probe the dielectric or piezoelectric properties of the sample at that particular DC bias. As already mentioned, the small-signal measurement of the capacitance (i.e. the permittivity) can be interpreted as a measure for the reversible response of the domain wall configuration present at a particular DC bias. The same line of arguments can be applied to the small-signal measurement of the piezoelectric coefficients. In this case, however, only the non-180° domain wall configuration is probed. By integration of the definition of the converse piezoelectric effect (in reduced notation)

$$x_j=d_{ij}E_i \quad (2)$$

it is therefore possible to obtain the reversible part of the strain component x_i. The matter, however, is slightly complicated by the fact that the strain–field dependence is not an analytical function of the field. A reversible strain-field dependence can nonetheless be constructed by resorting to an idealized butterfly loop and its relation to the derivative of the strain with respect to the field. From this relation it is clear what part of the small-signal d response corresponds to which part of the strain–field dependence. Using this information as a guideline, a butterfly loop can be reconstructed from an integrated d–E curve.

2. Experimental

The $PbZr_xTi_{1-x}O_3$ films of various Zr/Ti ratios were deposited by a 2-butoxyethanol based chemical solution deposition spin coating process. The butoxyethanol based precursor solution was synthesized by a modified method.[8,9] The films were deposited on standard commercial platinized Si-wafers [$Si/SiO_2/TiO_2/Pt$(100 nm)] from aixACCT Laboratories, Aachen, Germany. After each layer deposition, the films were pyrolized at 200 and 400 °C in air for 2 min each. The thickness of the films was varied by the number of deposition/pyrolysis cycles. After depositing the last layer the final crystallization was performed at 700 °C in O_2 with a rapid thermal annealing (RTA) process. Pt top electrodes of 100 nm were sputtered at room temperature and structured with a photolithography/lift-off process. A post-anneal to recover sputter-induced damages was performed at 700 °C in O_2.

The PZT ceramics investigated in this work were obtained from the University of Karlsruhe, Germany. More details on the samples can be found in Refs. 10 and 11. The samples were prepared using the mixed-oxide process. The ceramics were sintered at 1250 °C. Soft PZT ceramics with a neodymium dopant concentration of 2% $Pb_{0.97}Nd_{0.02}(Zr_xTi_{1-x}O_3$ were prepared. The zirconium content x was varied from $x=0.48$ (tetragonal) to $x=0.6$ (rhombohedral). The grain size of the ceramics varied between 3 and 4 μm and the relative density was always above 96% of the theoretical density.

The phase purity and crystallographic texture of the deposited films were determined by XRD using an X'PERT diffractometer (Phillips) with CuK_α radiation in Bragg-Brentano geometry. All thin films exhibited good phase purity. No second phases could be detected with X-ray diffraction analysis.

Most hysteresis curves presented in this work were measured with the aixACCT TF analyzer 2000, a computer based measurement tool to characterize ferroelectric thin films. The signal generation, amplification, A/D conversion, calculation and graphical representation were all performed with a desktop computer. The system allowed hysteresis measurements in the dynamical range between 1 Hz and 1 kHz with a maximal amplitude of 10 V.

In the same manner, ferroelectric bulk samples were characterized. In this case, however, a special high voltage probe head was used to protect the electronic circuits in case of a dielectric breakdown of the sample. The amplitude and frequency range was then determined by the high voltage amplifier used (Trek model 609D-6) whose input voltage was provided by the TF analyzer. With the Trek 609D-6, a maximal voltage of 4 kV could be applied to the sample. Due to the maximal current of 20 mA that this type of amplifier could drive, the upper limit of the dynamic range was just a few Hertz.

The capacitance–voltage dependence was measured with a HP 4284A LCR-bridge. The equipment used allowed the variation of the amplitude U_{AC} of the small-signal measuring signal between 5 mV and 10 V. By using the bias feature of the bridge, a DC voltage could be superimposed on the small measuring signal, thus allowing to measure the permittivity at different polarization states (which correspond to different points of the ferroelectric hysteresis). By changing the DC-bias in a step-like fashion, a complete C–V curve was measured. Since this measurement was controlled via the IEEE488 bus with a computer, the DC-bias could only be changed slowly, resulting in a large-signal frequency of approximately 100 mHz.

For higher frequencies of the large signal, a different method had to be used. Here, the slowly varying large signal was generated with an arbitrary waveform generator (Wavetek 395). On this signal, a small-signal measuring voltage (the reference channel of a Perkin-Elmer DSP model 7280 lock-in amplifier) was superimposed electronically. This signal was then fed to the sample. The answer of the sample was then applied to the input of the lock-in amplifier. With this setup a dynamic range of the large signal excitation between a few mHz up to 10 Hz was possible.

To measure the piezoelectric constants of bulk ceramics, a resonance method pioneered by Smits[12] has been used. Due to their piezoelectric activity, a ferroelectric material deforms periodically when subjected to an electric AC field. An electric field applied to a certain sample geometry (length >> width, thickness) along its thickness direction produces periodic deformations lengthwise. The piezoelectric constitutive equations read for this geometry:

$$x_1 = s_{11}^E X_1 + d_{31} E_3$$
$$D_3 = d_{31} X_1 + \varepsilon_{33}^X E_3 \quad (3)$$

The admittance of such a sample can be calculated in conjunction with Eq. (3) from the equation of motion of a deformable body of mass density ρ. For a sample of thickness d, length l and width b, the admittance can be shown to be:[12]

$$Y = \frac{i\omega lb}{d}\varepsilon_{33}^T - \frac{ib}{d}\left(\frac{\omega l}{s_{11}^E} - \frac{2}{s_{11}^E\sqrt{\rho s_{11}^E}}\tan\left(\frac{\omega l\sqrt{\rho s_{11}^E}}{2}\right)\right)d_{31}^2 \quad (4)$$

where ω is the angular frequency of the driving field. (A typical sample has the dimensions: $d = 500$ μm, $b = 2$ mm and $l = 14$ mm.)

By use of an iterative technique after Smits[12] a complete set of the complex small-signal parameters ε_{33}, d_{31} and s_{11} could be obtained by a single measurement.

In order to allow the determination of the material's parameters also under applied DC fields, a decoupling circuit was introduced which decoupled the high voltage source (Trek 609D-6) from the sensitive measurement bridge (HP 4192A). The setup was automatized using LabView since a single measurement at one particular DC bias took about 5 min to complete. The measurement equipment allowed the measurement of a d_{31}–V curve in approximately 5–6 h.

To measure strain-field ("butterfly") loops of bulk ceramics, the deformation $x1 = \Delta l_1/l_1$ as a function of the external field (applied along the x_3 direction) was recorded using an inductive position encoder based on a differential transformer of two coils. The primary coil was driven with an AC voltage of 11 kHz. The motion of a ferromagnetic core mechanically connected to the sample, induced different voltages into the coils due to the position dependent inductance. The voltage difference was directly proportional to the deformation Δl_1 of the sample and recorded with a digital oscilloscope for further evaluation.

The minute displacements (in the Ångstrøm range) of a ferroelectric thin film induced by an electric field can only be detected by making use of a laser interferometric technique. To measure the piezoelectric coefficient d_{33} and the strain–voltage dependence ("butterfly curve"), a double-beam laser interferometer was used. Since the electric field is applied parallel to the film normal, the induced strain variations cause a bending of the film substrate which reduces the resolution if only one laser beam is used to measure the deflection.[13] To eliminate these bending contributions, reflected beams (He–Ne laser $\lambda = 632.8$ nm) from both sides of the sample were brought to interference. For this purpose, the back of the substrate was polished to optical quality and coated with a reflective platinum film. The interference pattern of the beams was detected with a photodiode and fed to a lock-in amplifier (Perkin-Elmer DSP model 7280). The signal of the lock-in amplifier proportional to the displacement Δl was recorded with a digital oscilloscope (Tektronix, TDS 684C). Further details on the interferometer can be found in Refs. 13 and 14

Typical values of operation were: $U_{AC} = 200$ mV, $f_{AC} = 5$ kHz. d_{33} curves were measured with a large-signal frequency of 500 mHz, while strain–voltage curves were typically measured at 100 Hz.

3. Results

Fig. 1 displays the hysteresis curves and small-signal capacitance obtained for PZT thin films of various compositions. From the C–V curves, the reversible polarization was obtained by use of Eq. (1) and is shown in Fig. 2 for the different PZT compositions investigated. In the point of positive saturation the reversible polarization increased from 2.4 μC/cm^2 over 12.5 μC/cm^2 to 14.8 μC/cm^2 for the 30/70, 40/60 and 45/

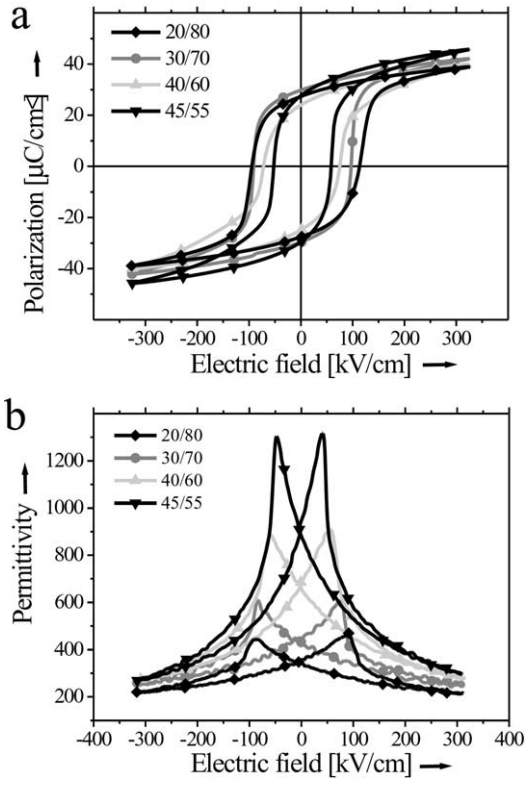

Fig. 1. (a) Hysteresis curves of PZT films of different composition (b) Relative permittivity as function of field for the same films (f_{AC} = 10 kHz). The frequency of the (triangular large) signal was 1 Hz for all measurements.

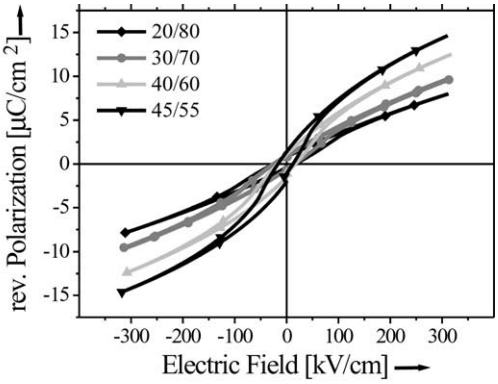

Fig. 2. Reversible polarization contributions for different PZT film compositions.

55 composition, respectively. The change of polarization of the hysteresis (i.e. the sum of reversible and irreversible contributions) in this composition range, however, is much smaller [Fig. 1(a)]. It can therefore be concluded that the reversible polarization contributions increase with decreasing Ti content (to be more precise, P_{rev} increases as the MPB is approached).

It is interesting to note that the extrinsic contributions in PZT films also increase as the MPB is approached. Hiboux et al. separated the domain wall from the intrinsic contributions to the permittivity by assuming

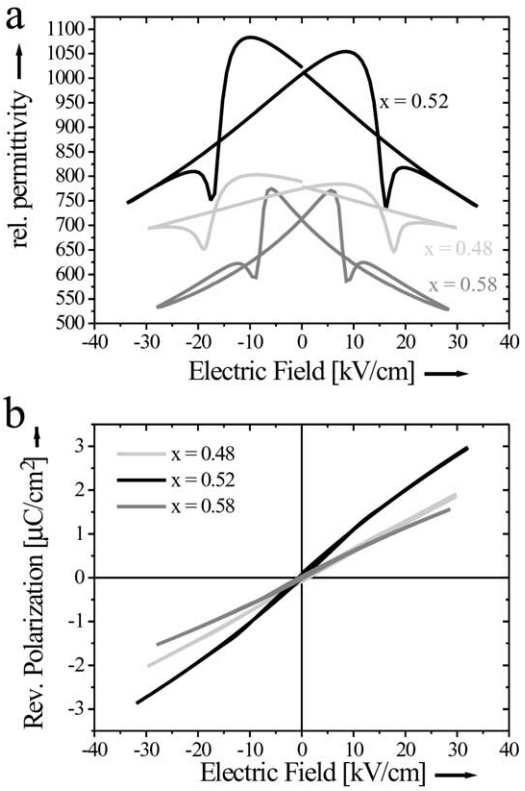

Fig. 3. (a) Relative permittivity and (b) reversible polarization of $PbZr_xTi_{1-x}O_3$ (2% Nd doped) samples.

that the permittivity at saturation is equal to the lattice contribution based on the notion that at this point all domain walls are driven out of the material.[15] The permittivity measured in excess of this value is then equal to the extrinsic contribution. It was observed that the domain wall contribution increased with decreasing Ti content and reached a maximum at the 45/55 composition (for higher Zr contents it decreased again). The data presented above is in complete agreement with their findings. For PZT compositions near the morphotropic phase boundary the domain wall density and/or mobility is thus significantly enhanced.

Analogous experiments were performed on $PbZr_xTi_{1-x}O_3$ bulk ceramics with compositions around the morphotropic phase boundary. Fig. 3(a) displays the relative permittivity as a function of DC-bias for a tetragonal ($x = 0.48$), a morphotropic ($x = 0.52$) and a rhombohedral ($x = 0.58$) sample. The highest permittivity was reached for the sample of composition close to the morphotropic phase boundary with $\varepsilon_r = 1013$. For the tetragonal and rhombohedral sample ε_r was determined to 783 and 711, respectively (at $E = 0$). The additional "humps" observed in the ε–E curves were also observed by others in ferroelectric ceramics and explained by different coercive fields for 180° and non-180° domains.[16] Their absence in ferroelectric thin films could be taken as evidence for suppressed non-180° domain switching in thin films.[17]

Fig. 3(b) shows the reversible polarization contributions determined by integration of the capacitance–voltage curves of Fig. 3(a). The result is very similar to the one observed for the thin film samples. The highest reversible contributions were observed for the morphotropic composition, while the tetragonal and rhombohedral samples exhibited smaller reversible polarization contributions. From this perspective, thin films and bulk ceramics show the same qualitative behavior. However, a difference was observed when the magnitude of the reversible polarization was related to the total polarization. Fig. 4 shows a comparison of the reversible polarization to the total polarization for bulk ceramics (a) and thin films (b). It can clearly be seen that while in bulk ceramics the reversible contribution to the total polarization is almost negligible, it amounts to almost one third in thin film samples.

TEM studies of PZT 20/80 thin films and bulk ceramics showed that the 90° type domain morphology is to first order similar for both systems. However, the mobility of 90° domain walls is greatly reduced in thin films.[18] Atomic force microscopy (AFM) studies on epitaxial PZT films showed that 90° domain walls form a complicated network that inhibits the motion of single walls.[19,20] In view of the presented results, it is therefore suggested that a large part of the ferroelectric response of thin films is due to reversible domain wall motion, i.e. bending of otherwise immobile domain walls while in bulk ceramics the walls are easily moved by the application of an external field.

Another evidence that non-180° domain wall processes in ferroelectric thin films are strongly suppressed becomes clear by measuring the dielectric high frequency behavior in the GHz range. In ferroelectric bulk ceramics, the reversible dielectric small signal response consists of (a) intrinsic, (b) 180° domain wall and (c) non-180° domain wall contributions. At high frequencies only the parts (a) and (b) are still operating. The mechanism is caused by the fact that a vibrating non-180° wall acts as an emitter of elastic shear waves propagating with the shear wave velocity through the grain. When the frequency of the applied electric field corresponds to shear wave velocity the vibration of the domain wall is suppressed and a strong dielectric relaxation is observed, as shown in Fig. 5. In ferroelectric thin films, the relaxation step is not found.

The response of the domain walls contributes considerably to the dielectric and piezoelectric properties of a ferroelectric material. While both 180° and non-180° walls contribute to the permittivity, only non-180° walls affect the piezoelectric response of a ferroelectric. A displacement of a 180° wall does not change the strains and thus yields no piezoelectric response. A comparison between dielectric and piezoelectric properties of a material can therefore provide information about what type of walls are involved in a phenomena.

For this reason, piezoelectric measurements on thin films and bulk ceramics were performed. The piezoelectric coefficient, d_{33}, and strain component, x_3, were determined of a PZT 45/55 thin film of 300 nm thickness with a double-beam interferometer. The piezoelectric response, d_{31}, of a PZT bulk ceramic ($x=0.58$) was measured using the resonance method. The strain-voltage dependence was determined with an inductive position encoder.

Fig. 6(a) shows a butterfly loop of a PZT ceramic ($x=0.58$) measured at 16 mHz and Fig. 6(b) displays the transverse piezoelectric coefficient d_{31} of the same sample. (The large-signal DC bias was changed at a rate of 10 V/min.) The observed value for d_{31} at $E=0$ of

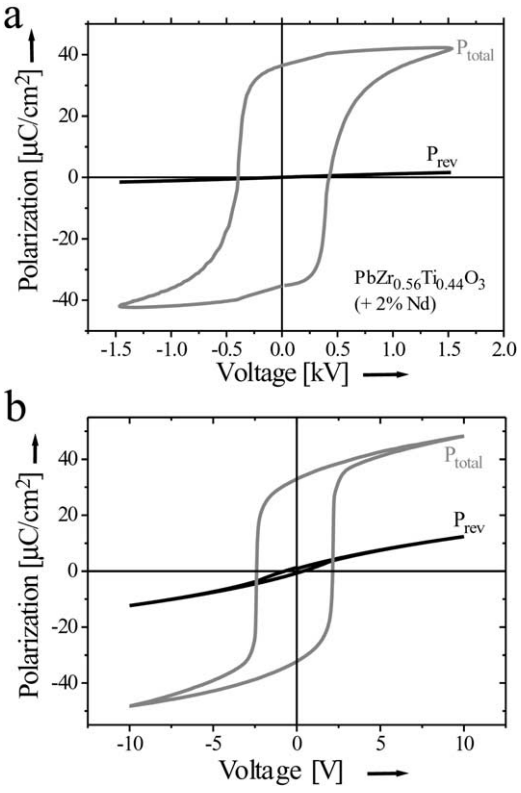

Fig. 4. Comparison of total polarization to reversible polarization for a PZT ($x=0.56$) ceramic (a) and a thin film (45/55) (b).

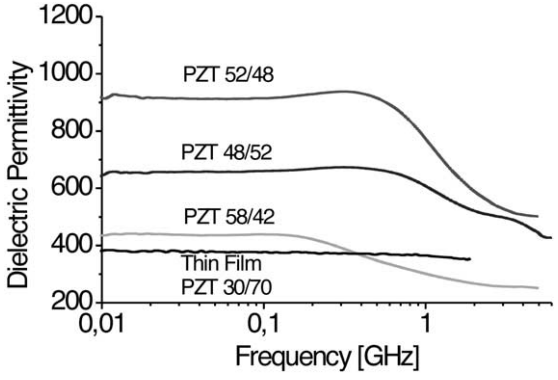

Fig. 5. Frequency dependence of the dielectric permittivity for bulk ceramics of various compositions and a thin film sample.

68×10^{-12} C/N is consistent with literature reports for PZT of the same composition.[21]

An example of such a reversible butterfly loop in comparison to the large-signal measured butterfly loop is shown in Fig. 7. Notice that the slope of the strain-voltage dependence in the saturation regime is identical to the slope of the integrated d dependence in saturation. To illustrate this finding, a line with the slope of the integrated d curve was drawn on top of the saturation regime of the large-signal butterfly loop. In the saturation regime, the response of the material was solely determined by the response of the lattice since at this high fields all domain walls should have been driven out of the material, in complete analogy to the discussion of the reversible polarization. Thus, in this regime the slope of the large-signal measurement and the reversible strain curve should be identical which was indeed observed. An important difference, however, is that the reversible strain curve was smaller than the large-signal butterfly loop. From this data it can be inferred that in the point of saturation approximately one third of the large-signal strain was due to reversible processes. The reader might object that both curves were measured at different frequencies (16 and 0.05 mHz for the butterfly loop and d_{31} loop, respectively). However, this manifests itself mainly by the position of the "switching peak" as can be inferred from Fig. 8, showing different strain–voltage curves for three different frequencies. The two butterfly loops measured with low frequencies (16 and 200 mHz) only deviated regarding the position of the "switching peak" which shifted outwards for higher frequencies (in complete agreement with the frequency dependence of the coercive field E_c). However, the magnitude of the strain change was the same for both frequencies.

Indeed, in the saturation regime both curves were identical. For higher frequencies, not only the switching peak position was shifted outwards, but also the height of the curves decreased which could partly, however, be attributed to the inertia of the measurement setup. During a strain-voltage curve measurement, the sample was mechanically in contact with a piston that transformed a change of position into a voltage via an inductive mechanism. For high frequencies, this piston could not follow the length change of the sample anymore. Thus, had the butterfly loop shown in Fig. 7 been also measured at 0.05 mHz, the resulting curve would be very similar to the one shown except for the position of the switching peak. Therefore, the argument presented above remains intact.

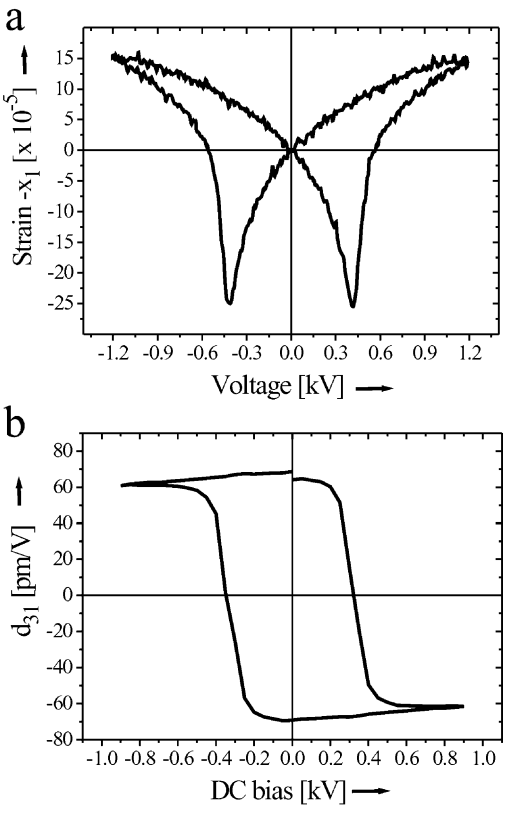

Fig. 6. (a) Strain–field dependence of a $PbZr_{0.58}Ti_{0.42}O_3$ bulk ceramic (2% Nd doped); (b) d_{31} dependence on electric field of the same sample.

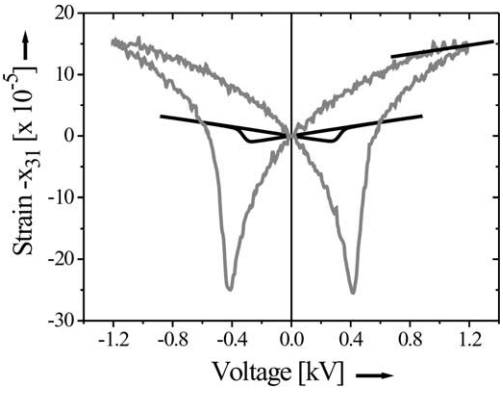

Fig. 7. Comparison of integrated d_{31} curve (black) with butterfly loop (gray) of a PZT bulk ceramic ($x=0.58$).

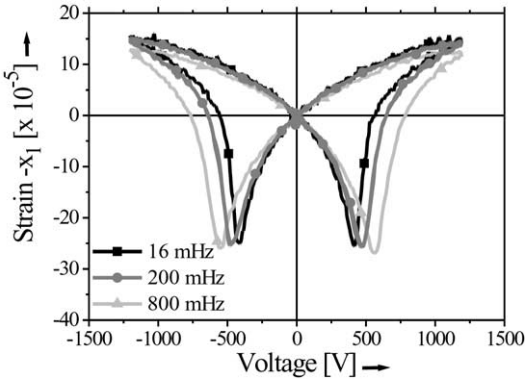

Fig. 8. Strain–voltage curves of a PZT bulk ceramic ($x=0.58$) at different frequencies of the large signal.

Analogous measurements were also performed on a PZT 45/55 thin films (thickness 300 nm). The strain–voltage curves and the d_{33}-voltage dependence were measured with a double-beam interferometer. The results are displayed in Fig. 9. The measured small-signal piezoelectric constant d_{33} was in agreement with other values reported in literature for films of this composition.[22] The reversible strain curve (black curve in Fig. 9b) was constructed analogously to the bulk ceramic case. The difference to bulk ceramics is striking if this curve is compared to the butterfly loop measured on the same film. About 80% of the strain response of the film appeared to originate from reversible processes. The fact that both curves were measured at different frequencies impacts this statement only slightly which was detailed for the bulk ceramics case already. Had the butterfly curve also been measured at 500 mHz, the overall shape would just be slightly different (mainly the position of the switching peak). The frequency dependence of the butterfly curve basically manifests itself in the switching peak position not in the overall appearance of the loop.[14]

The reversible contribution to the polarization in ferroelectric thin films was also found to be enhanced in this work. Since the polarization response of the film was determined by both 180° and non-180° domain wall motion and the piezoelectric response was solely due to non-180° boundaries, the presented results are evidence that most reversible domain wall motions in ferroelectric thin films are due to reversible motion of non-180° domain walls. The clamping effect of the substrate which entails rather stringent mechanical boundary conditions apparently only allows for minute motions of the non-180° walls, which immediately return to their initial positions when the external electric field that initiated the motion is returned to zero.

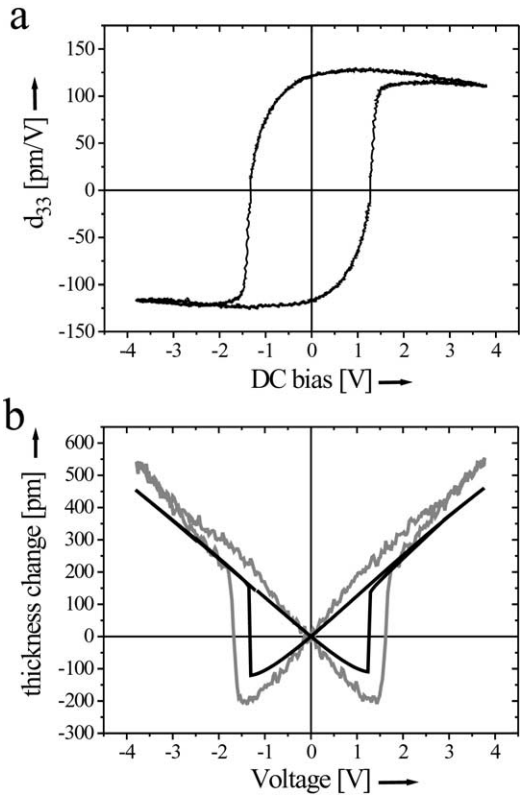

Fig. 9. Piezoelectric coefficient d_{33} (a) (f = 500 mHz, f_{AC} = 2 kHz, U_{AC} = 200 mV) and "Butterfly" loop (b) measured at 100 Hz and the integrated d_{33} response of a PZT 45/55 film.

4. Conclusions

The novel characterization method of using integrated small-signal properties of ferroelectrics to characterize reversible processes was applied to the piezoelectric and polarization response of ferroelectric ceramics and thin films. The investigation revealed a much higher reversible contribution in thin films compared to bulk ceramics, for both ferroelectric and ferroelastic properties, indicating that non-180° walls are responsible for the enhanced reversible contributions in thin films. This finding provides further evidence for a limited non-180° domain wall mobility in thin films.

Acknowledgements

The authors would like to thank Dr. C. Heilig and Professor Dr. K.H. Härdtl of the Institut für Werkstoffe der Elektrotechnik, University of Karlsruhe for providing the PZT bulk ceramics samples and the Deutsche Forschungsgemeinschaft for financial support.

References

1. Zhang, Q., Pan, W., Jang, S. and Cross, L., Domain wall excitations and their contributions to the weak-signal response of doped lead zirconate titanate ceramics. *J. Appl. Phys*, 1988, **64**, 6445.
2. Damjanovic, D., Stress frequency dependence of the direct piezoelectric effect in ferroelectric ceramics. *J. Appl. Phys*, 1788, **82**, 1997.
3. Taylor, D. and Damjanovic, D., Evidence of domain wall contribution to the dielectric permittivity in PZT thin films at subswitching fields. *J. Appl. Phys*, 1973, **82**, 1997.
4. Damjanovic, D. and Demartin, M., Contributions of the irreversible displacement of domain wall to the piezoelectric effect in barium titanate and lead zirconate titanate ceramics. *J. Phys. Condens. Matter*, 1997, **9**, 4943–4953.
5. Bolten, D., Böttger, U. and Waser, R., Reversible and irreversible polarization processes in ferroelectric ceramics and thin films. *J. Appl. Phys*, 1735, **93**, 2003.
6. Bozorth, R., *Ferromagnetism*, 3rd edn. Van Nostrand, New York, 1955.
7. Cammarano, R., McCormick, P. and Street, R., The interrelation of reversible and irreversible magnetization. *J. Phys. D: Appl. Phys*., 1996, **29**, 2327–2331.
8. Budd, K., Dey, S. and Payne, D., Sol-gel processing of $PbTiO_3$,

$PbZrO_3$ and PZT thin films. *Brit. Ceram. Soc. Proc.*, 1985, **36**, 107–121.
9. Nouwen, R., Mullens, J., Franco, D., Yperman, J. and Poucke, L. C., Use of thermogravimetric analysis-Fourier transform infrared spectroscopy in the study of the reaction mechanism of the preparation of Pb(Zr, Ti)O_3 by the sol-gel method. *Vibrational Spectroscopy*, 1996, **10**, 291.
10. Schäufele, A. and Härdtl, K., Ferroelastic properties of lead zirconate titanate ceramics. *J. Am. Ceram. Soc.*, 1996, **79**, 2637–2640.
11. Heilig, C. and Härdtl, K., Time dependence of mechanical depolarization in ferroelectric ceramics. *Proc. 11th IEEE Symposium on Applications of Ferroelectrics*, 1998, **596**, 504–506.
12. Smits, J., Iterative method for accurate determination of the real and imaginary part of the materials coefficients of piezoelectric ceramics. *IEEE Trans. Sonics and Ultrasonics*, 1976, **23**, 393–402.
13. Kholkin, A. L., Wüterich, C., Taylor, D. V. and Setter, N., Interferometric measurements of electric field-induced displacements in piezoelectric thin films. *Review of Scientific Instruments*, 1996, **67**, 1935–1942.
14. Gerber, P., *Aufbau und Erprobung eines Doppelstrahl-Laser-Interferometers zur Charakterisierung von ferroelektrischen Dünnschichten*. Rheinisch-Westfälische Technische Hochschule Aachen, Germany, 2001.
15. Hiboux, S., Muralt, P. and Maeder, T., Domain and lattice contributions to dielectric and piezoelectric properties of $Pb(Zr_x,Ti_{1-x})O3$ thin films as function of composition. *J. Mater. Res.*, 1999, **14**, 4307–4318.
16. Bar-Chaim, N., Brunstein, M., Grünberg, J. and Seidman, A., Electric field dependence of the dielectric constant of PZT ferroelectric ceramics. *J. Appl. Phys.*, 1974, **45**, 2398–2405.
17. Damjanovic, D., Ferroelectric, dielectric and piezoelectric properties of ferroelectric thin films and ceramics. *Rep. Prog. Phys.*, 1998, **61**, 1267–1324.
18. Tuttle, B., Headley, T., Drewien, C., Michael, J., Voigt, J. and Garino, T., Comparison of ferroelectric domain assemblages in $Pb(Zr,Ti)O_3$ thin films and bulk ceramics. *Ferroelectrics*, 1999, **221**, 209–218.
19. Lee, K., Choi, J., Lee, J. and Baik, S., Domain formation in epitaxial $Pb(Zr,Ti)O_3$ thin films. *J. Appl. Phys.*, 2001, **90**, 4002–4095.
20. Ganpule, C., Nagarajan, V., Hill, B., Roytburd, A., Williams, E., Ramesh, R., Alpay, S., Roelofs, A., Waser, R. and Eng, L., Imaging three-dimensional polarization in epitaxial polydomain ferroelectric thin films. *J. Appl. Phys.*, 2002, **91**, 1477–1481.
21. Jaffe, B., Cook, W. and Jaffe, H., *Piezoelectric Ceramics*. Academic Press, London, 1971.
22. Taylor, D., *Dielectric and Piezoelectric Properties of Sol-gel Derived $Pb(Zr,Ti)O_3$ Thin Films*. PhD Thesis, Ecole Polytechnique Fédérale de Lausane, 1999.